Supplementary Information

Organelle-like structural evolution of coacervate droplets induced by photopolymerization

Mei Zhu, Zhenhui Li, Junbo Li, Youping Lin, Haixu Chen, Xin Qiao, Xiaoliang Wang Xiaoman Liu and Xin Huang**

MIIT Key Laboratory of Critical Materials Technology for New Energy Conversion and Storage, School of Chemistry and Chemical Engineering
Harbin Institute of Technology
Harbin, 150001, P. R. China
E-mails: liuxiaoman@hit.edu.cn; xinhuang@hit.edu.cn

Supplementary Figures

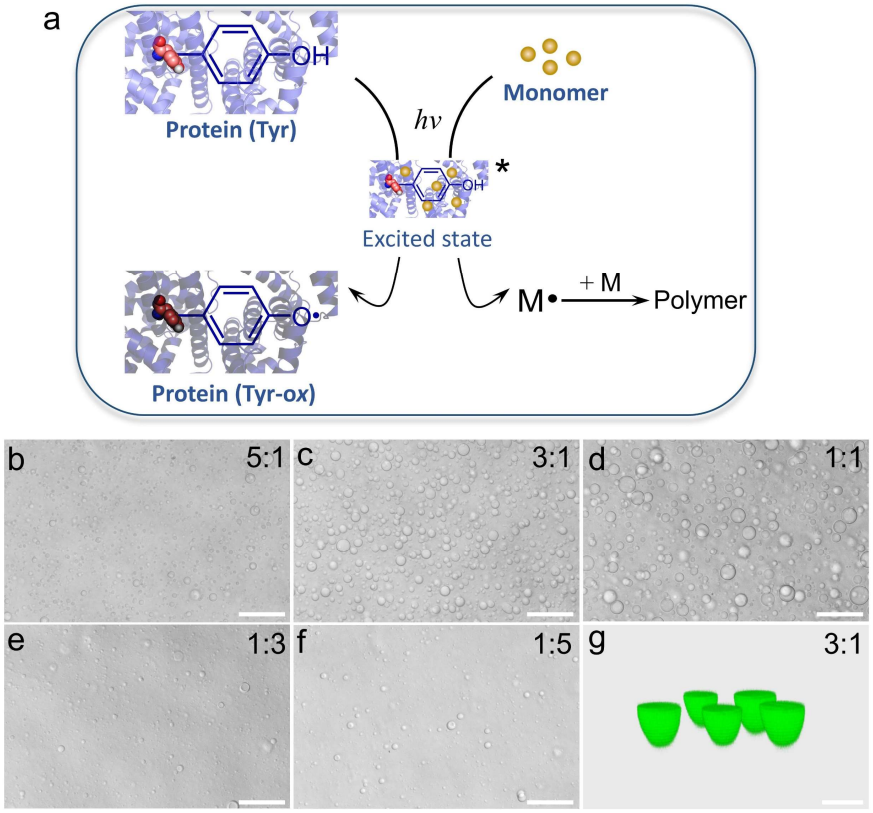

Supplementary Fig. 1. (a) Schematic illustration of BSA-mediated photopolymerization. The main polymerization process is that excited-state protein under light irradiation could enhance its reduction ability significantly, and then protein and monomer undergo electron transfer to generate primary free radicals, which subsequently initiate chain propagation to synthesize polymer. (b-f) Microscopy images of coacervates formed at the different volume ratio of HA/PDDA. HA = 15 mg/mL, PDDA = 85 mg/mL. The volume ratio of HA/PDDA = 3:1 is used for the following experiments. (g) 3D image of HA/PDDA coacervates (volume ratio, 3:1), green fluorescence from calcein. Scale bars, 50 μm.

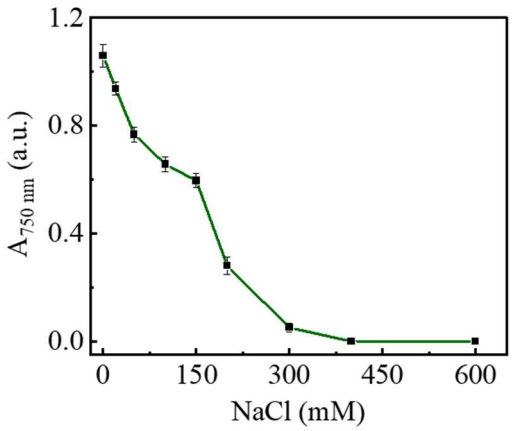

Supplementary Fig. 2. Turbidity measurements (Absorbance = 750 nm) of HA/PDDA coacervates under the different concentrations of NaCl in H_2O. Data are presented as mean ± s.d. (n = 3). Source data are provided as a Source Data file.

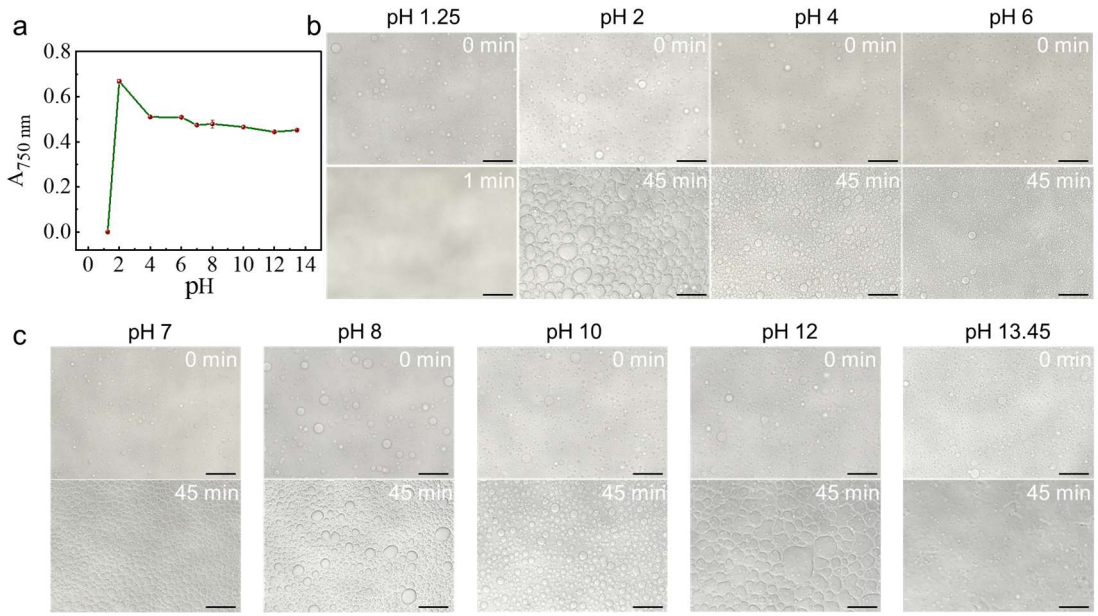

Supplementary Fig. 3. (a) Turbidity measurements of HA/PDDA coacervates in PBS buffer with programming pH (20 mM) (Absorbance at 750 nm). Data are presented as mean ± s.d. (n = 3). (b, c) The corresponding microscopy images of HA/PDDA coacervates at 0 min and 45 mins. The results indicate that the coacervate is unstable at pH = 1.25 and remains stable within the pH range of 2-12. Scale bars, 50 μm. Source data are provided as a Source Data file.

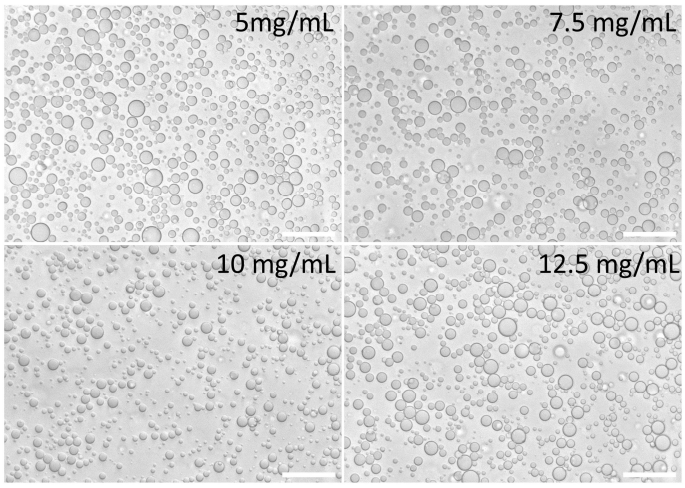

Supplementary Fig. 4. Microscopy images of HA/PDDA coacervates with the presence of the different concentrations of BSA. Scale bars, 50 μm.

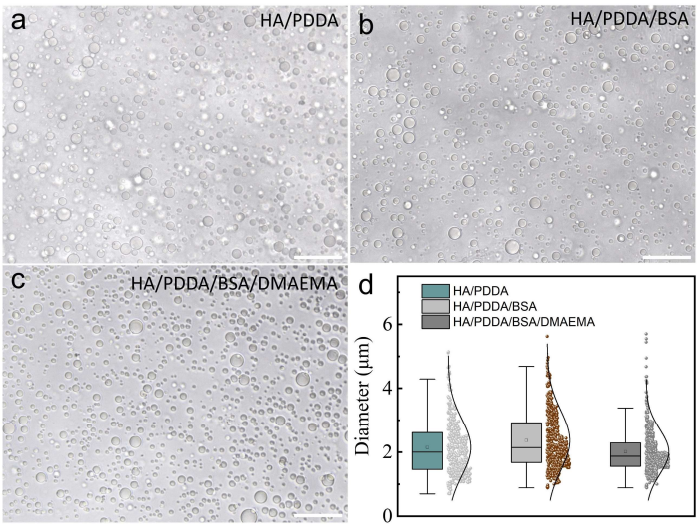

Supplementary Fig. 5. Microscopy images of (a) HA/PDDA coacervates, (b) HA/PDDA/BSA coacervates and (c) HA/PDDA/BSA/DMAEMA coacervates. (d) The corresponding diameter statistics shown in (a-c). HA/PDDA coacervates are prepared at the volume ratio of HA/PDDA = 3:1 (HA = 15 mg/mL, PDDA = 85 mg/mL). BSA (7.5 mg/mL) and DMAEMA (5% w/v) are added. Data are presented as mean ± s.d. (n = 367). Scale bars, 20 μm. Source data are provided as a Source Data file.

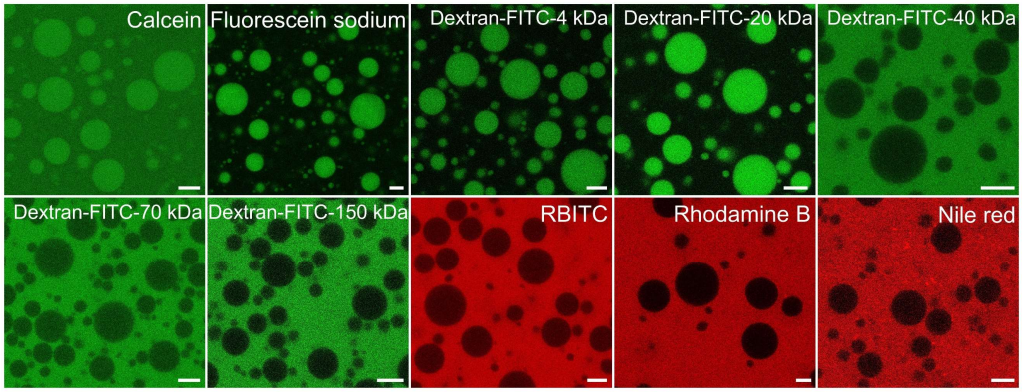

Supplementary Fig. 6. CLSM images of the sequestration and size exclusion of HA/PDDA/BSA/DMAEMA coacervates (0 h) for dyes. The negative dye molecules (calcein, fluorescein sodium) are sequestrated while positive dyes (RBITC, Rhodamine B), hydrophobic dye Nile red and dextran-FITC with a molecular weight over 40 kDa are excluded. Scale bars, 5 μm.

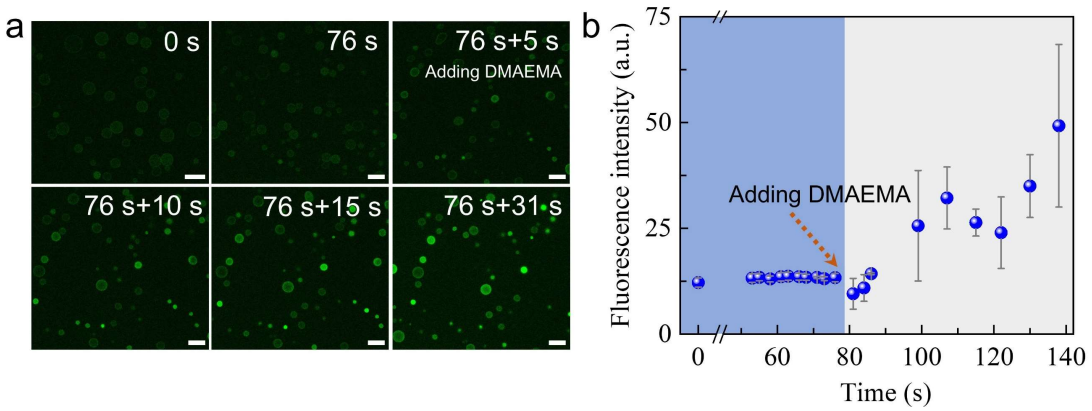

Supplementary Fig. 7. DMAEMA facilitates encapsulation of BSA into HA/PDDA coacervates. (a) Time-dependent CLSM images of HA/PDDA coacervates encapsulating BSA-FITC, showing that the process is facilitated by adding DMAEMA, (BSA-FITC, green fluorescence). (b) The corresponding fluorescent statistics of HA/PDDA coacervates after adding BSA-FITC and DMAEMA. Data are presented as mean ± s.d. (n = 3). Scale bars, 10 μm. Source data are provided as a Source Data file.

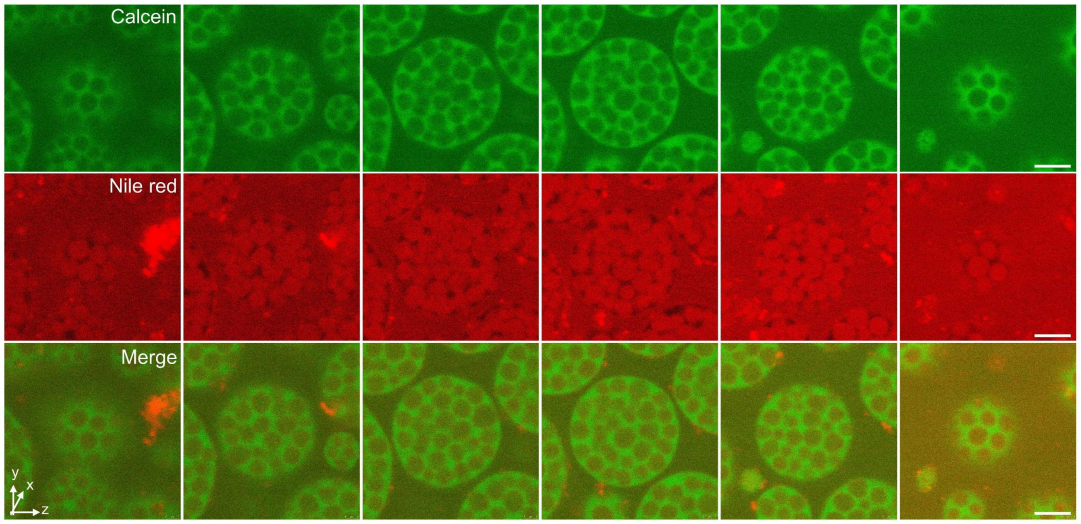

Supplementary Fig. 8. CLSM images of multi-compartmental coacervates along the z-direction formed by 405 nm illumination for 2.5 h, showing the three-dimensional characteristic of compartmentalization and the different spatial sequestration. Calcein (green) is sequestrated in the coacervate matrix and Nile red (red) is encapsulated in sub-compartments. Scale bars, 3 μm.

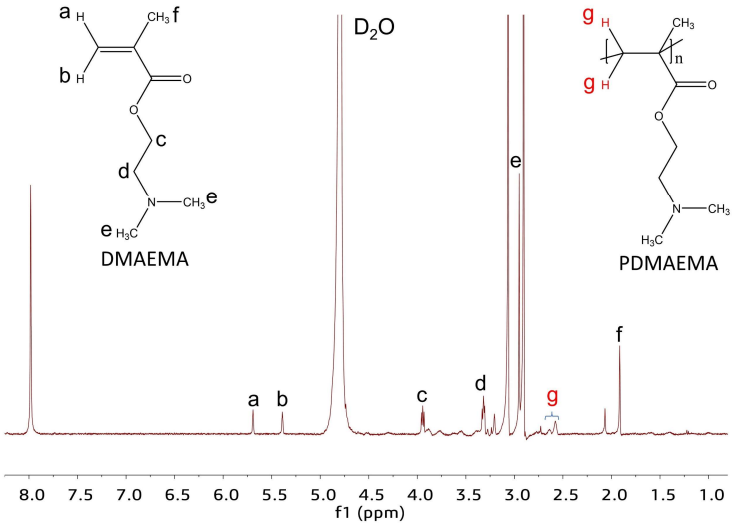

Supplementary Fig. 9. ^{1}H NMR spectrum of photopolymerization coacervate phase at 2.5 h in D_2O. HA/PDDA/BSA/DMAEMA coacervates was carried out at 405 nm at room temperature for 2.5 h, and then centrifuged at 5300 × *g* for 10 min. The precipitation was diluted with D_2O of 600 mM NaCl for ^{1}H NMR spectrum. New proton signals of -CH_2- on alkane chain at δ = 2.58 ppm marked as g, revealing the generation of PDMAEMA. Source data are provided as a Source Data file.

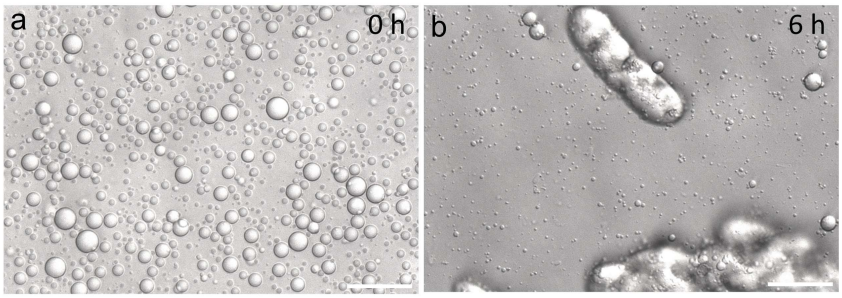

Supplementary Fig. 10. Microscopy images of HA/PDDA/BSA coacervates without illumination observed at (a) 0 h and (b) 6 h. Dissociation and coalescence of the coacervate occur within 6 h. Scale bars, 50 μm.

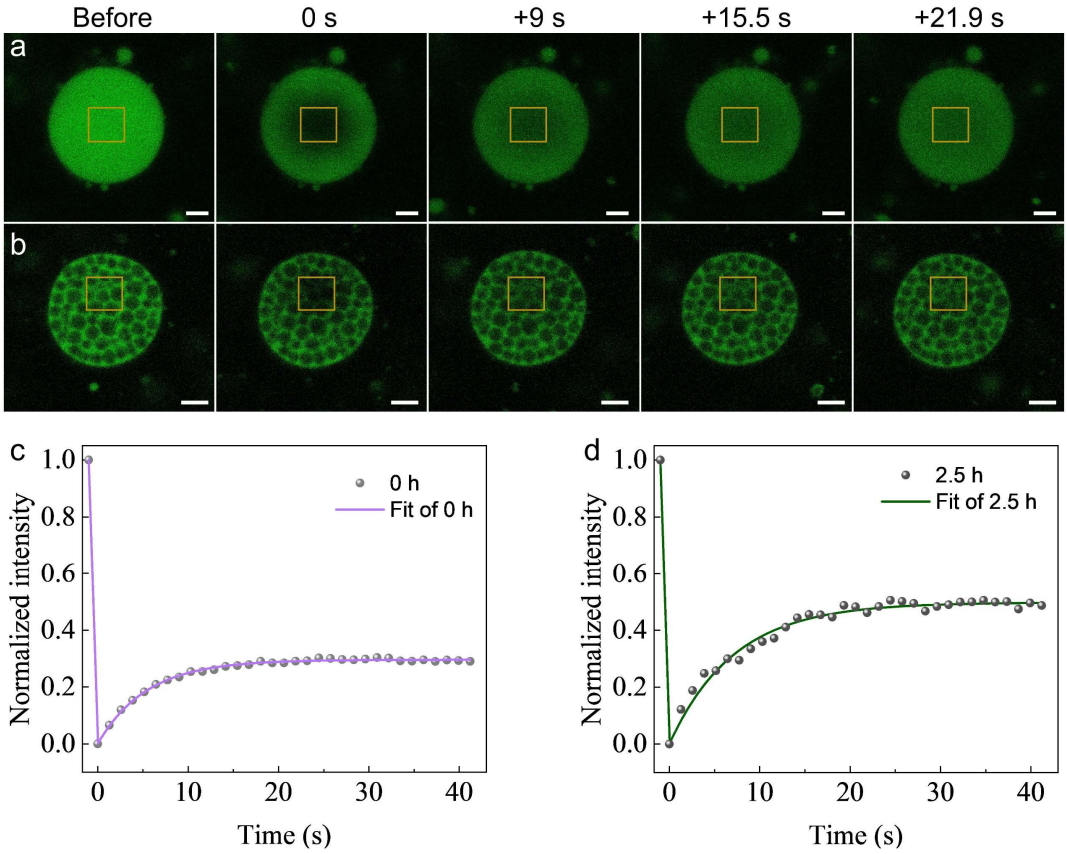

Supplementary Fig. 11. CLSM images of FRAP experiment of HA/PDDA/BSA/DMAEMA coacervates: (a) 0 h, (b) polymerization under 405 nm illumination for 2.5 h. HA labelled by 5-AF (green fluorescence). (c, d) The corresponding fluorescent recovery plot in (a) and (b), respectively. The multi-compartmental coacervates formed by 405 nm illumination for 2.5 h, show fine mobility similar to the original coacervates (0 h), and the fluorescence are recovered within 20 seconds. Scale bars, 3 μm. Source data are provided as a Source Data file.

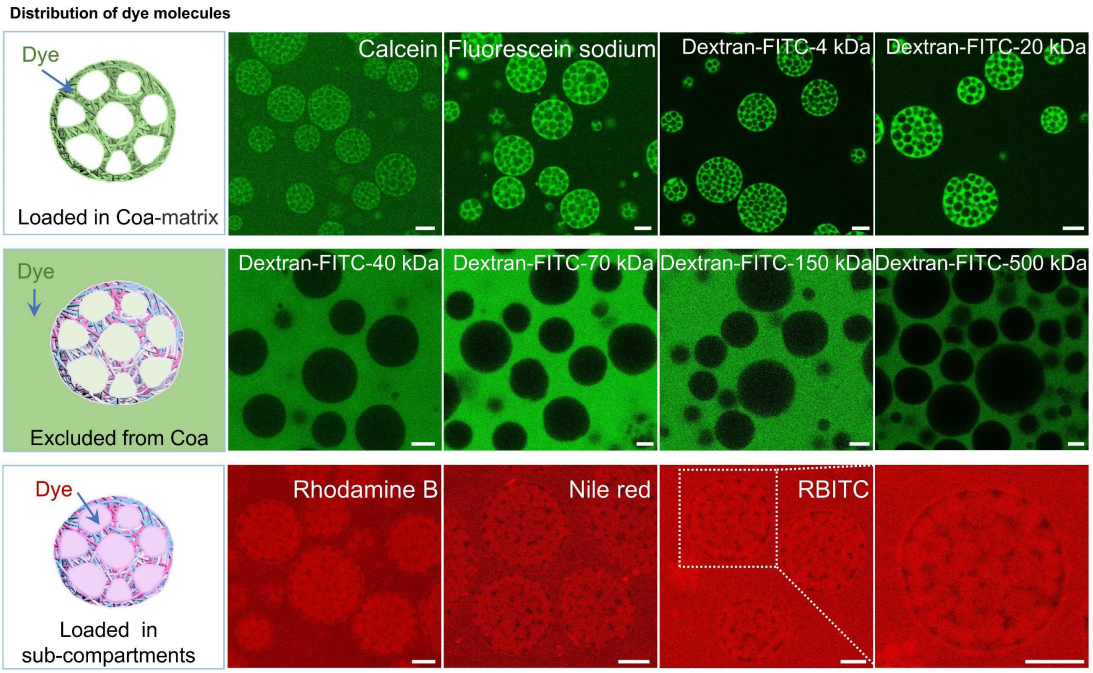

Supplementary Fig. 12. CLSM images of sequestration of multi-compartmental coacervates for dyes. The multi-compartmental coacervates are formed by illumination under 405 nm for 2.5 h. The dyes including calcein, fluorescein sodium, dextran-FITC-4 kDa and dextran-FITC-20 kDa are sequestered into the matrix, and dextran-FITC with a molecular weight over 40 kDa is excluded. The molecules including rhodamine B, Nile red, and RBITC are encapsulated in sub-compartments. Scale bars, 5 μm.

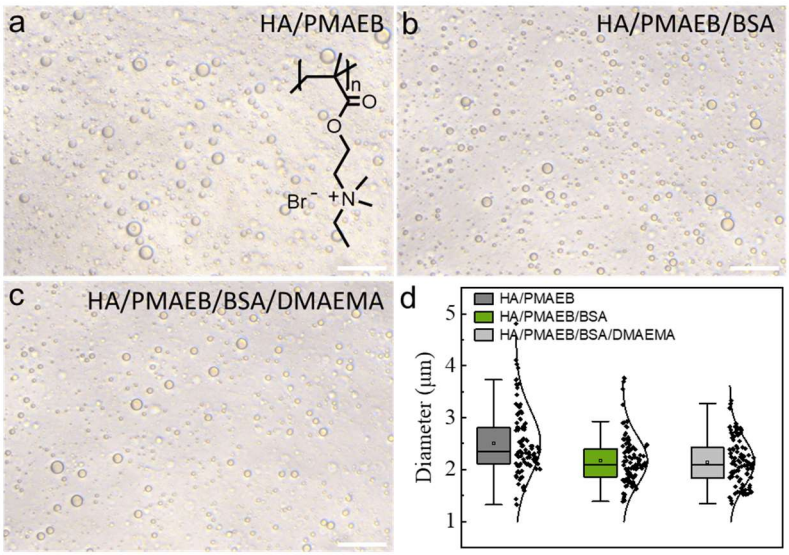

Supplementary Fig. 13. Microscopy images of (a) HA/PMAEB coacervates, (b) HA/PMAEB/BSA coacervates, (c) HA/PMAEB/BSA/DMAEMA coacervates. (d) The corresponding statistics of diameter in (a-c). Data are presented as mean ± s.d. (n = 92). Scale bars, 20 μm. Source data are provided as a Source Data file.

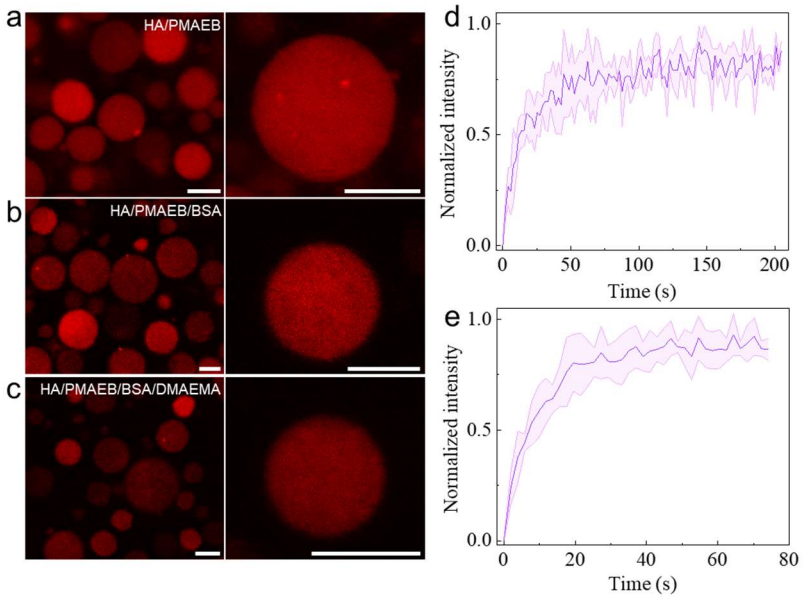

Supplementary Fig. 14. CLSM images of (a) HA/PMAEB coacervates, (b) HA/PMAEB/BSA coacervates, (c) HA/PMAEB/BSA/DMAEMA coacervates. Red fluorescence is from PMAEB-RBITC. The inset in (a) is the molecular structure of PMAEB. The fluorescence intensity recovery plot of (d) HA/PMAEB coacervates and (e) HA/PMAEB/BSA coacervates, showing liquid-like characteristic of coacervates. The shaded region represents the error interval of standard deviation of the mean points (n=3). Scale bars, 3 μm. Source data are provided as a Source Data file.

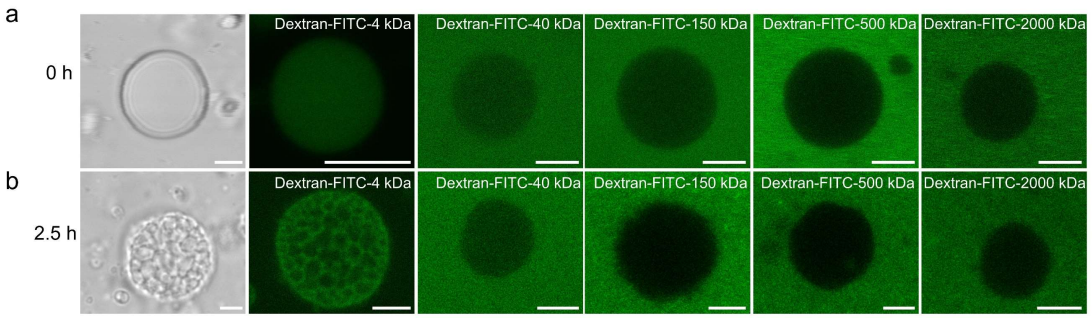

Supplementary Fig. 15. CLSM images of HA/PMAEB/BSA/DMAEMA coacervates encapsulating dextran-FITC. The coacervate are obtained by 405 nm illumination for (a) 0 h and (b) 2.5 h. Dextran-FITC-4 kDa is sequestered into the matrix, and dextran-FITC with a molecular weight over 40 kDa is excluded. Scale bars, 3 μm.

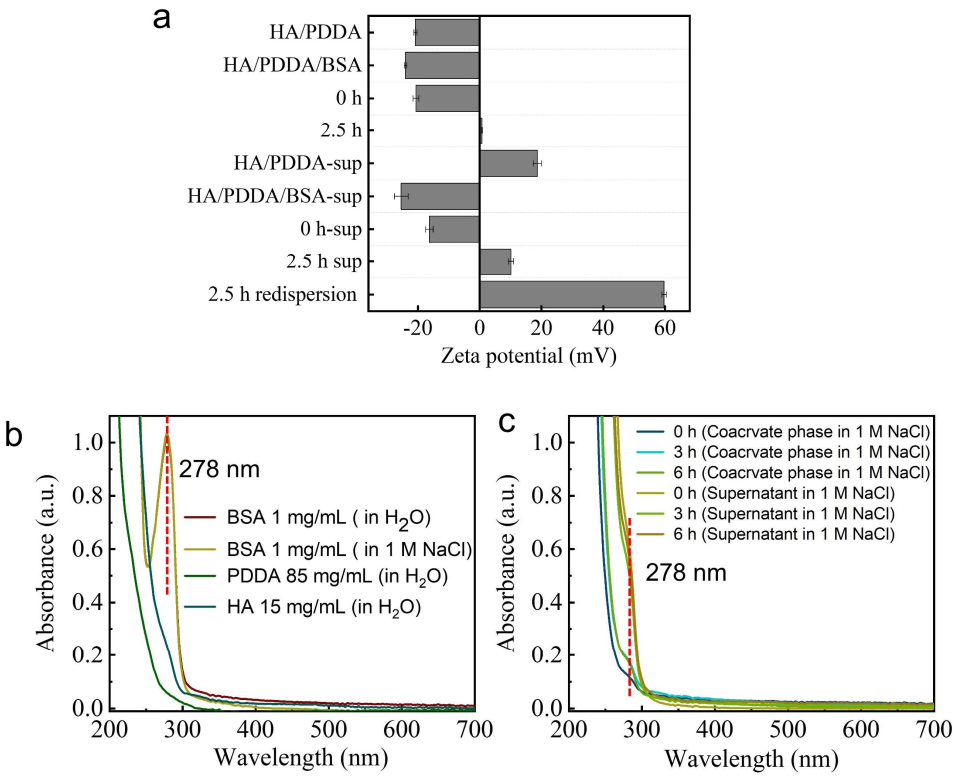

Supplementary Fig. 16. (a) Zeta potential of HA/PDDA coacervates, HA/PDDA/BSA coacervates, HA/PDDA/BSA/DMAEMA coacervates (0 h), multi-compartmental coacervates obtained by 405 nm illumination for 2.5 h (2.5 h) and the corresponding supernatant. For obtaining the zeta potential of the multi-compartmental coacervate, 2.5 h redispersion is prepared by resuspending the multi-compartmental coacervate (2.5 h) in H_2O after centrifugation. The measurement is carried out in H_2O at 25°C. Data are presented as mean ± s.d. (n = 3). The zeta potential of bulk solution increased from -16.3 ± 1.22 mV (0 h-sup) to a positive potential 10.1 ± 0.73 mV (2.5 h-sup) after polymerization for 2.5 h, which indicated the generation of PDMAEMA in bulk solution. (b) UV-Vis absorption spectrum of BSA, PDDA and HA in H_2O or NaCl (1 M). The maximum absorption of BSA is at 278 nm. (c) UV-Vis absorption spectrum of the coacervate phase and the corresponding supernatant (bulk solution) at different polymerization times in NaCl (1 M). The absorbance at 278 nm indicates that the bulk solution contains BSA. Source data are provided as a Source Data file.

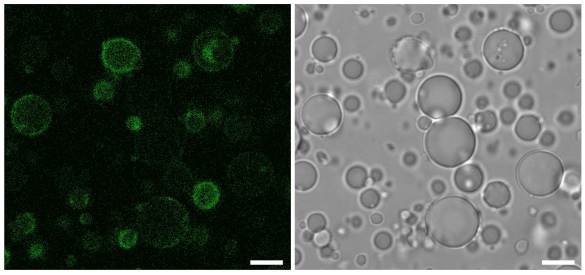

Supplementary Fig. 17. CLSM images of HA/PDMAEMA/PDDA/BSA coacervates showing the spatial distribution of PDMAEMA. PDMAEMA labelled with fluorescein O-methacrylate (green fluorescence). PDMAEMA-FMA is mainly located around the periphery of coacervates phase. Scar bars, 5 μm.

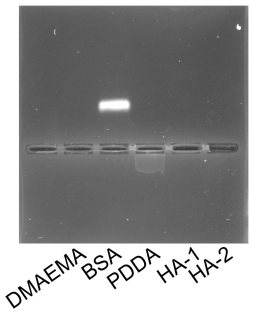

Supplementary Fig. 18. Agarose gel electrophoresis of DMAEMA, BSA, PDDA, HA, running time, 20 min. DMAEMA: 25 w/v, BSA: 7.5 mg/mL, PDDA: 12.75 mg/mL, HA-1: 5.25 mg/mL, HA-2:15 mg/mL. Source data are provided as a Source Data file.

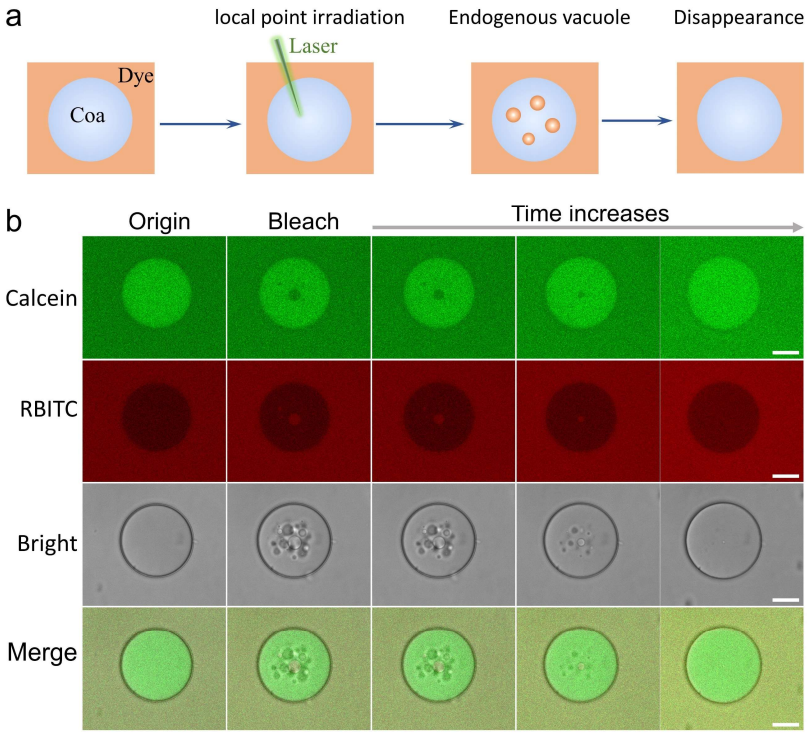

Supplementary Fig. 19. (a) Schematic illustration showing that local point irradiation in HA/PDDDA/BSA/DMAMEA coacervates induces the formation of vacuoles. (b) CLSM images of HA/PDDA/BSA/DMAEMA coacervates encapsulating calcein (green) and taking in RBTIC (red) from external solution due to the formation of endogenous vacuoles, indicating that internal driving force is an important factor in the formation of multi-compartmental coacervates. Scale bars, 3 μm.

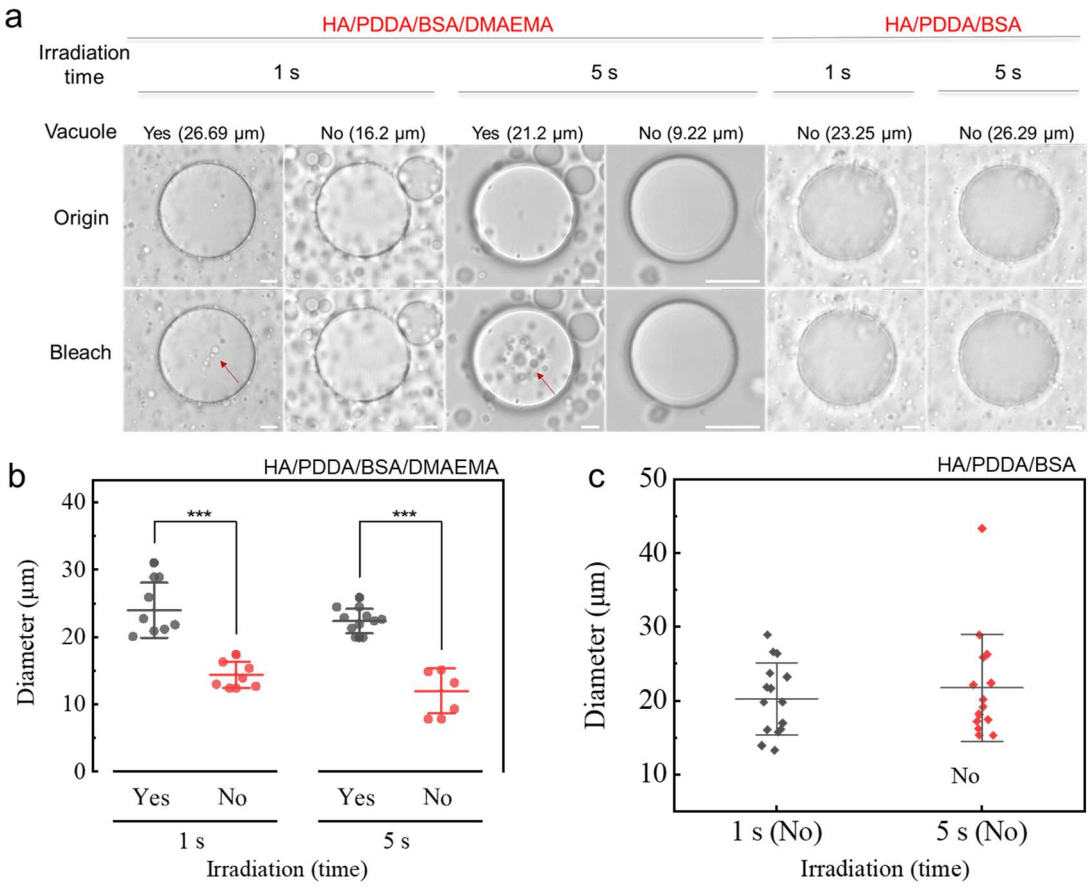

Supplementary Fig. 20. (a) CLSM images of HA/PDDA/BSA/DMAEMA coacervates and HA/PDDA/BSA coacervates after local point irradiation (Bright channel). (b, c) Plots of the diameter of coacervates versus vacuole event after 1 s or 5s irradiation: (b) HA/PDDA/BSA/DMAEMA coacervates, (c) HA/PDDA/BSA coacervates. Yes: vacuoles occur, No: no vacuoles. Local point irradiation in HA/PDDDA/BSA/DMAMEA coacervates induces the formation of vacuoles, and large-sized coacervates are more likely to induce vacuoles. As a control experiment, HA/PDDA/BSA coacervates does not generate the vacuoles. HA/PDDA coacervates are prepared at the volume ratio of HA/PDDA = 3:1 (HA = 15 mg/mL, PDDA = 85 mg/mL). BSA (7.5 mg/mL) and DMAEMA (5% w/v) are added. HA labelled by 5-aminofluorescein (HA-AF). Data are presented as mean ± s.d. (n=15), * p<=0.05, ** p<=0.01, *** p<=0.001. Scale bars, 5 μm. Source data are provided as a Source Data file.

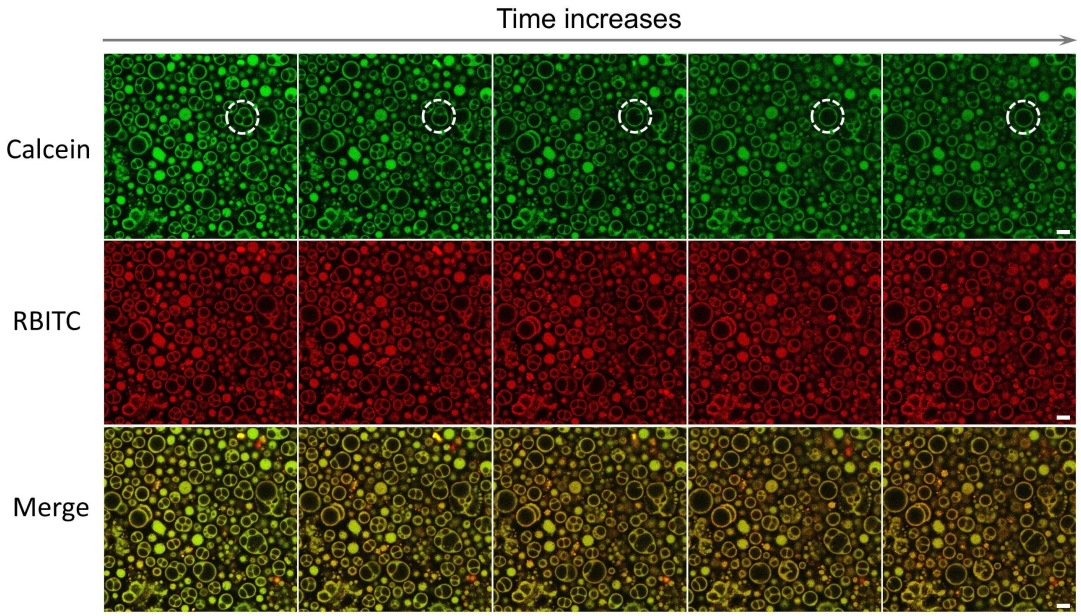

Supplementary Fig. 21. Time-dependent CLSM images of the deformation process of multi-compartmental coacervates induced by resuspending the centrifugal multi-compartmental coacervates into H_2O. The multi-compartmental coacervates are formed by 405 nm illumination for 5 h. Scale bars, 5 μm.

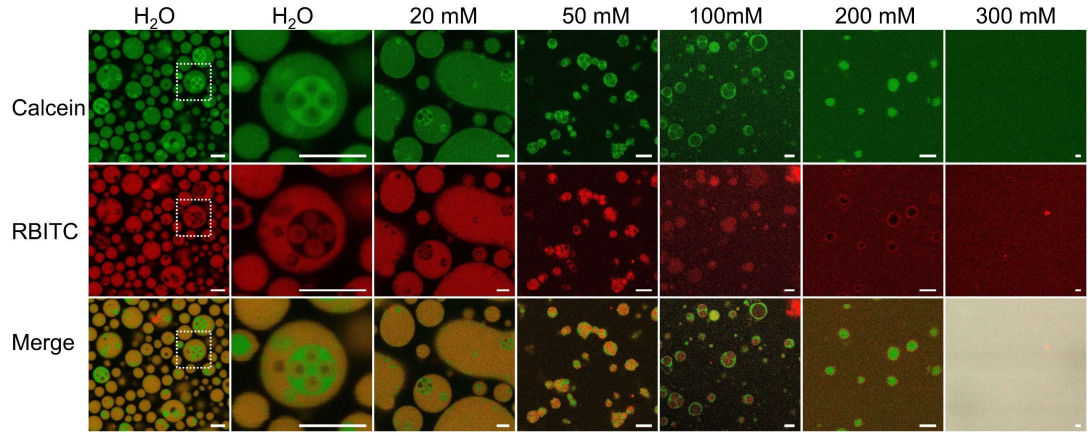

Supplementary Fig. 22. NaCl-dependent CLSM images of HA/PDDA/BSA/DMAEMA coacervates formed by 405 nm illumination for 2.5 h (5% w/v content). Generally, 10 μL of the multi-compartmental coacervate solution was added with 50 μL of NaCl solution. Scale bars, 5 μm.

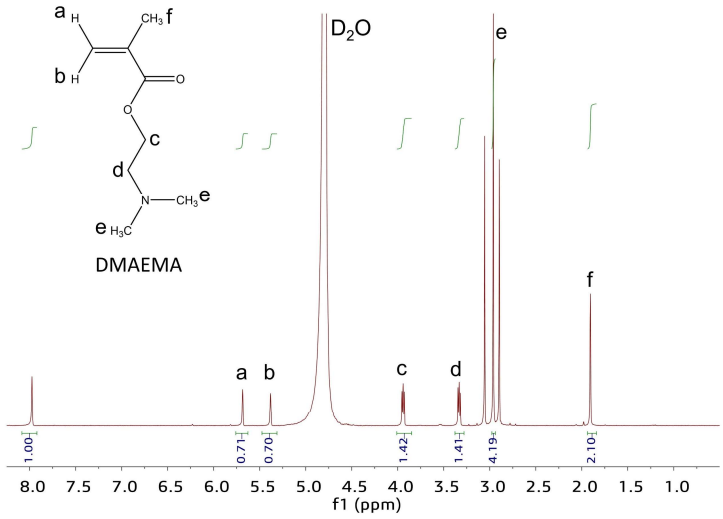

Supplementary Fig. 23. ^{1}H NMR spectrum of photopolymerization supernatant at 0 h in D_2O. HA/PDDA/BSA/DMAEMA coacervates is centrifuged at 5300 × *g* for 10 min. The supernatant is diluted with D_2O of 600 mM NaCl for ^{1}H NMR spectrum. The obvious proton signals of DMAEMA were marked as a-f, indicating that bulk phase contained DMAEMA. Source data are provided as a Source Data file.

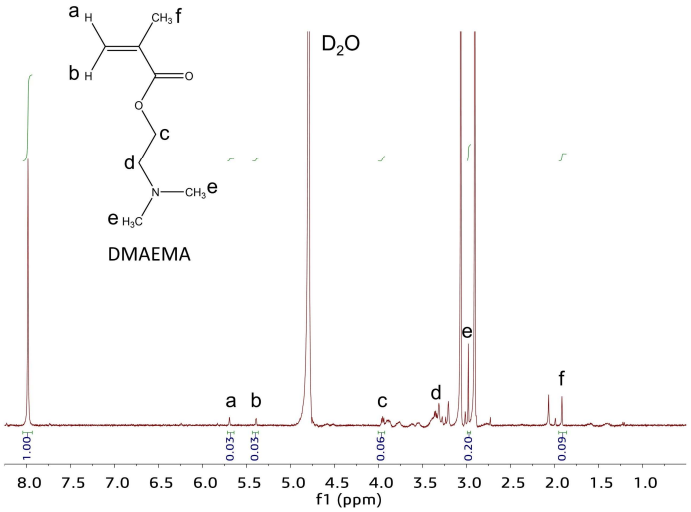

Supplementary Fig. 24. ^{1}H NMR spectrum of photopolymerization coacervate phase at 0 h in D_2O. HA/PDDA/BSA/DMAEMA coacervates is centrifuged at 5300 × *g* for 10 min. The precipitation is diluted with D_2O of 600 mM NaCl for ^{1}H NMR spectrum. The proton signals of DMAEMA were marked as a-f, indicating that DMAEMA was encapsulated into HA/PDDA/BSA coacervates. Source data are provided as a Source Data file.

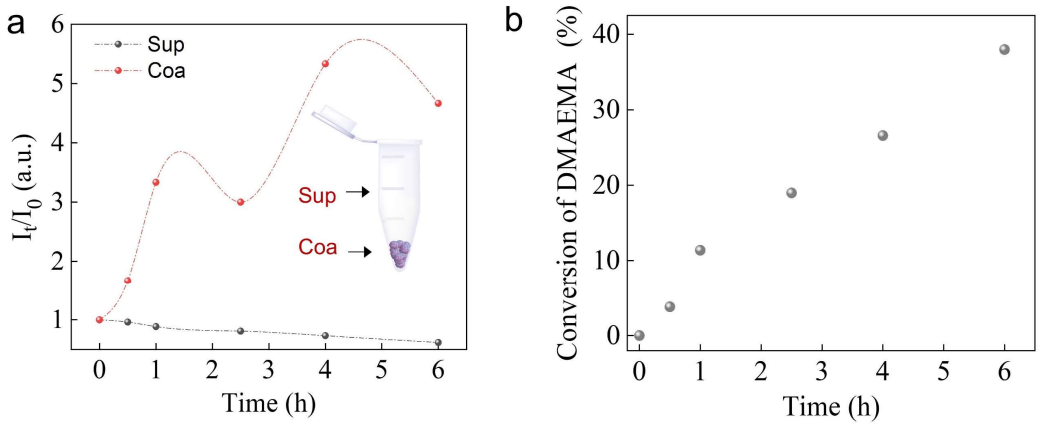

Supplementary Fig. 25. (a) Plots of DMAEMA ratio in sediment (coacervate phase) or supernatant versus photopolymerization time. (b) The plot of conversion ratio of DMAEMA versus time in HA/PDDA/BSA/DMAEMA bulk solution. Conversion ratio of DMAEMA = (1- I_t/I_0)*100%, where I_t and I_0 correspond to integral of signal at 5.69 ppm at different hours and 0 hours attributed to proton signals of H-C=C- of DMAEMA. ^{1}H NMR is performed in D_2O. Source data are provided as a Source Data file. According to the conversion rate of DMAEMA, we estimate osmotic pressure differences of bulk solution with time as follows. Approximating the osmotic pressure Π in bulk phase as that for a dilute ideal solution[1,2].

$$\Pi = cRT \qquad \text{equation (1)}$$

where Π is the osmotic pressure, c is the molar concentration, R is the ideal gas constant, and T is the temperature (K). We approximately calculate the osmotic pressure difference for bulk solution as:

$$\triangle\Pi = (C_t\text{-}C_0)\ RT \qquad \text{equation (2)}$$

After photopolymerization for 2.5 h under 405 nm, the estimated osmotic pressure difference is about -137.2 kPa, and after photopolymerization for 6 h, osmotic pressure difference is estimated to be -274.42 kPa. Decreasing osmotic pressure of bulk solution is beneficial for the formation of the internal sub-compartments. The bulk solution of the multi-compartment coacervates, formed after polymerization for 6 hours, is replaced by water, and the estimated osmotic pressure difference will increase to about -388.73 kPa, which will lead to the fusion between the sub-compartments.

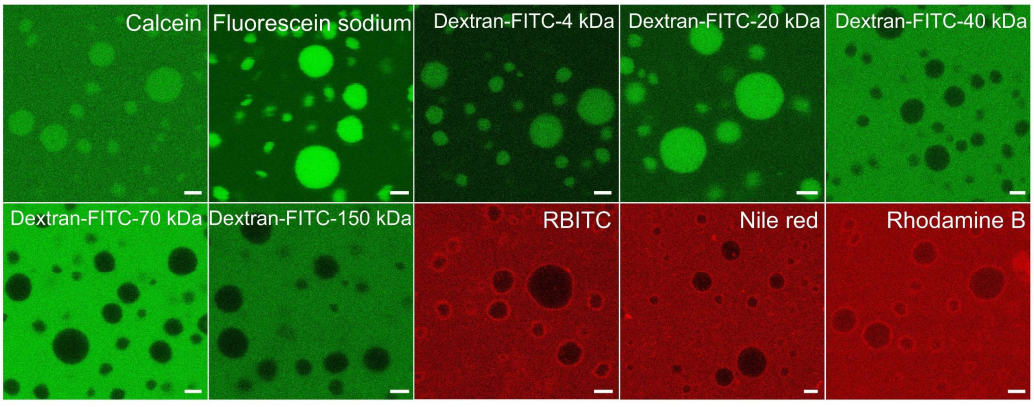

Supplementary Fig. 26. CLSM images of sequestration of dyes in the final decubation coacervates. The dyes including calcein, fluorescein sodium, dextran-FITC-4 kDa and dextran-FITC-20 kDa are sequestered into the interior of the final coacervates. Dextran-FITC with a molecular weight over 40 kDa is excluded. The small molecule dyes including Nile red, RBITC, rhodamine B are distributed at the outer membrane and bulk solution of coacervates. This final coacervate matrix showed the similar encapsulation behavior to original HA/PDDA/BSA/DMAEMA coacervates (0 h). Scale bars, 3 μm.

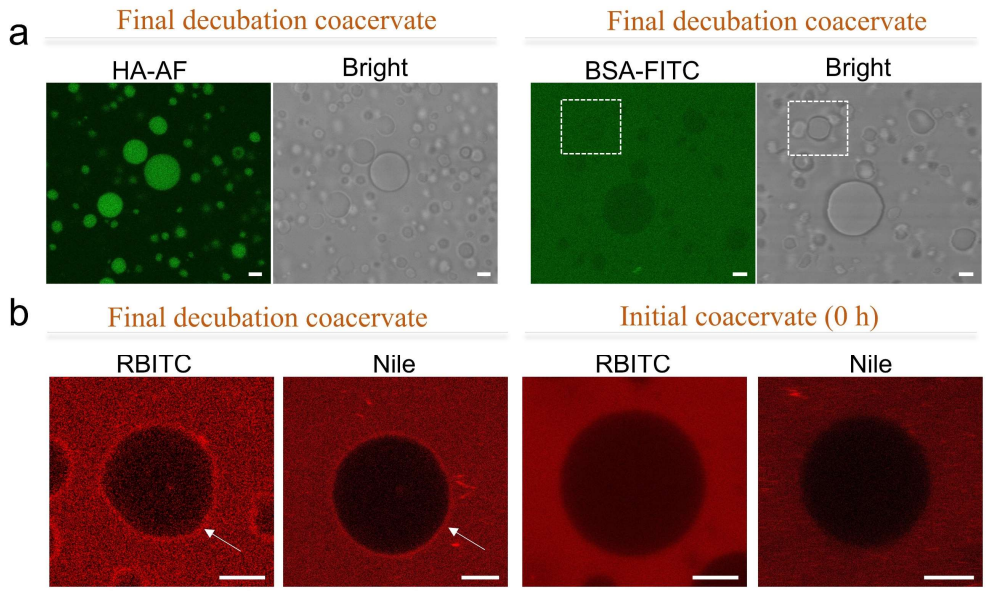

Supplementary Fig. 27. (a) CLSM images of distribution of HA and BSA in the final coacervate after decubation process. HA-AF and BSA-FITC show green fluorescence. The results indicate that HA is distributed in the interior of coacervates. Similarly, the detention of BSA by coacervates is a slow process, but BSA can still be distributed inside coacervates as shown in the white box in (a). (b) CLSM images of distribution of RBITC and Nile in the final decubation coacervates and the initial coacervate (0 h). Compared with the initial coacervate, the final decubation coacervates show a distinct red fluorescent around outer membrane (white arrows), indicating that the polymer is not only distributed in bulk solution, but also on the outer membrane of the final decubation coacervates. Scale bars, 3 μm.

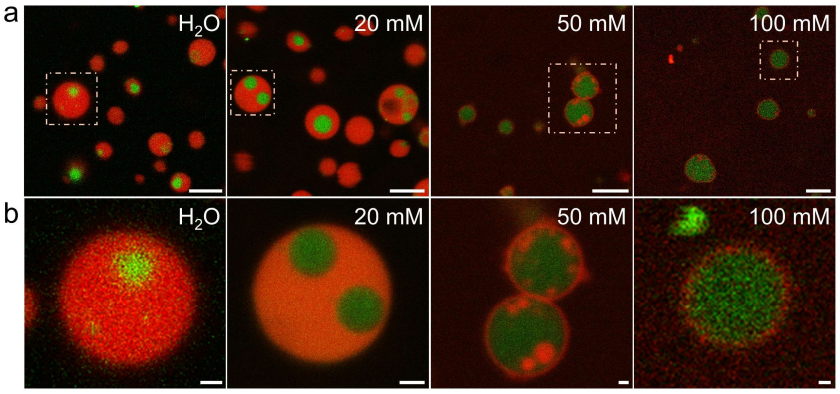

Supplementary Fig. 28. (a) NaCl-dependent CLSM images of the reconstructed coacervates (HA/PDDA/BSA/DMAEMA) formed by 405 nm illumination for 6 h (10% w/v content). Generally, 10 μL of reaction solution was added with 190 μL of NaCl solution of different concentrations, scale bars, 5 μm. (b) The corresponding zoom images in (a), (HA-AF, green) (Nile red, red). Scale bars, 1 μm. The reconstructed coacervates showed two phases. HA was distributed in inner phase, and the external phase showed encapsulation of Nile red.

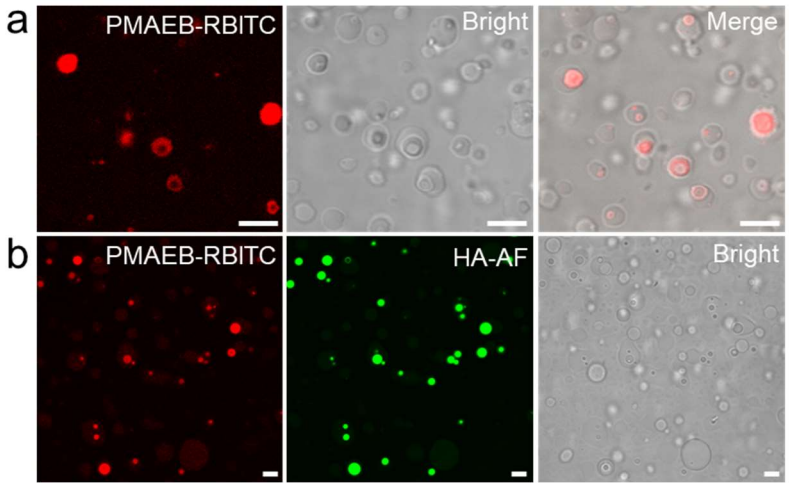

Supplementary Fig. 29. The investigation of the spatial distribution of PMAEB in reconstructed coacervates. (a) CLSM images of the reconstructed HA/PMAEB/BSA/DMAEMA coacervates, showing that PMAEB-RBITC was distributed in inner phase. (b) CLSM images of the reconstructed HA/PMAEB/BSA/DMAEMA coacervates adding with HA-AF in-situ, showing that both PMAEB-RBITC and HA-AF were distributed in inner phase. The formed process of external reconstructed coacervates: the coacervates (HA/PMAEB/BSA/DMAEMA) is formed by 405 nm illumination for 6 h, and 10 μL of reaction solution was added with 190 μL of aqueous solution. Scar bars, 5 μm.

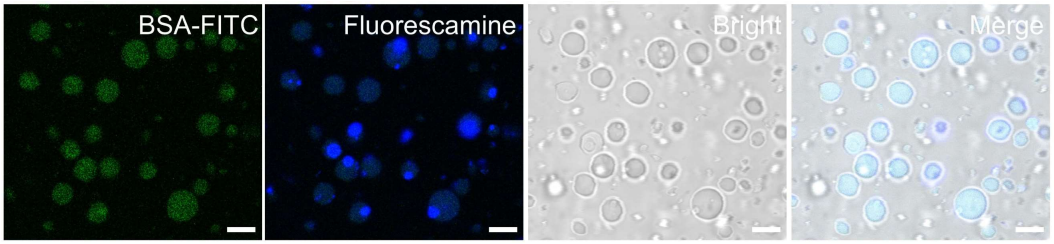

Supplementary Fig. 30. The investigation of the spatial distribution of BSA in reconstructed coacervates. CLSM images of the reconstructed HA/PDDA/BSA/DMAEMA coacervates, and BSA was labelled by FITC and fluorescamine, respectively. Fluorescamine can quantitatively interact with the primary amino groups of amino acids and proteins to form stable, high fluorescence, and low background complexes under mild conditions. BSA labelled by fluorescamine showed strong blue fluorescence in inner phase. According to the above investigation, these results indicated that the internal phase composition of reconstructed coacervates was HA/PDDA/BSA, and the external phase composition of reconstructed coacervates was BSA/PDMAEMA. The formed process of the reconstructed coacervates: the coacervates (HA/PMAEB/BSA/DMAEMA) is formed by 405 nm illumination for 6 h, and 10 μL of reaction solution was added with 190 μL of aqueous solution. Scar bars, 5 μm.

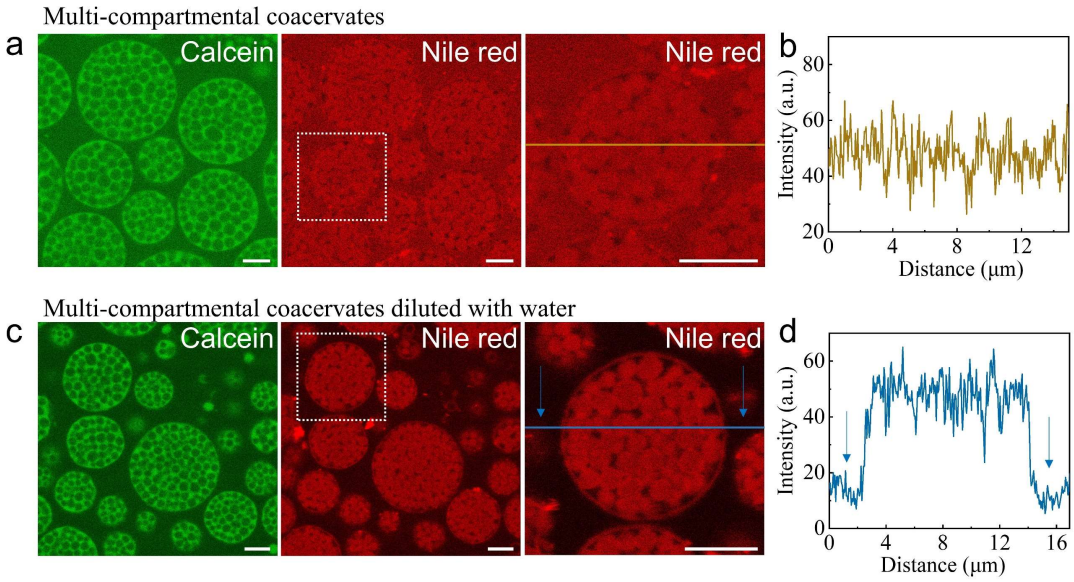

Supplementary Fig. 31. (a) CLSM images of the distribution of calcein (green) and Nile red (red) in multi-compartmental coacervates. (b) The corresponding line fluorescence intensity in (a) showing that the sub-compartments and bulk solution present the similar distribution of dyes. (c) CLSM images of the distribution of calcein (green) and Nile red (red) in multi-compartmental coacervates diluted with H_2O. (d) The corresponding line fluorescence intensity in (c) showing that the multi-compartmental coacervates are formed by illumination under 405 nm for 2.5 h. Dilute the multi-compartmental coacervates with twice the volume of water to obtain the diluted multi-compartmental coacervates. The blue arrows in (c, d) indicate the decreased red fluorescent intensity of bulk solution. Scale bars, 5 μm. Source data are provided as a Source Data file.

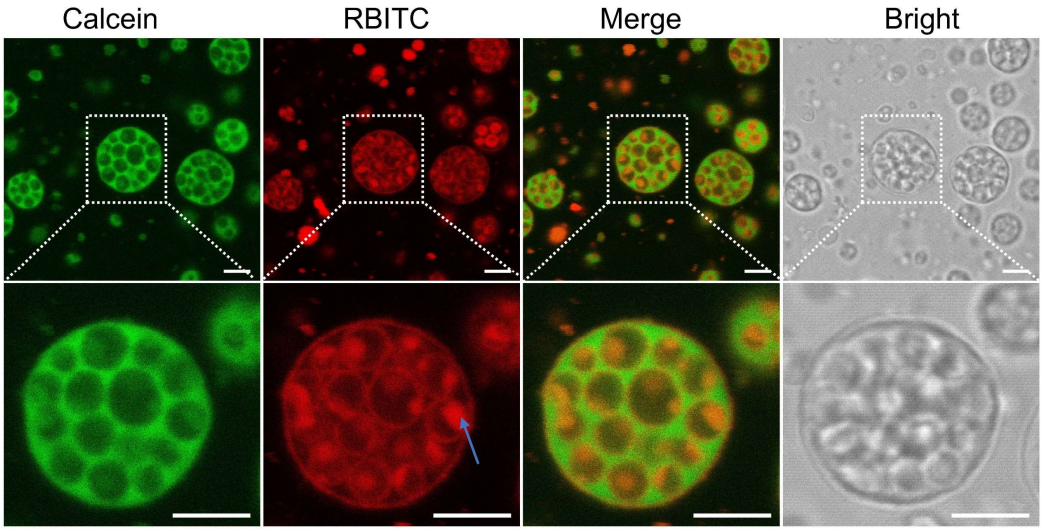

Supplementary Fig. 32. CLSM images of the resuspended multi-compartmental coacervates in H_2O after centrifugation at 530 × *g* for 1min, showing that BSA/PDMAEMA phase (RBITC, red) is distributed in the sub-compartments as indicated by a blue arrow. The multi-compartmental coacervates are formed by 405 nm illumination for 2.5 h. Scale bars, 5μm.

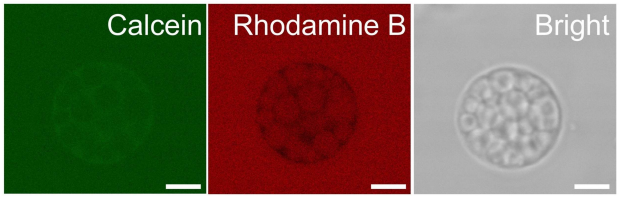

Supplementary Fig. 33. CLSM images of sequestration of multi-compartment coacervates after 70 days for calcein/rhodamine B. Calcein (green) is sequestrated in the coacervate matrix. Rhodamine B (red) is encapsulated in sub-compartments. The multi-compartment coacervate is formed by 405 nm illumination for 2.5 h and applied after 70 days. Scar bars, 3 μm.

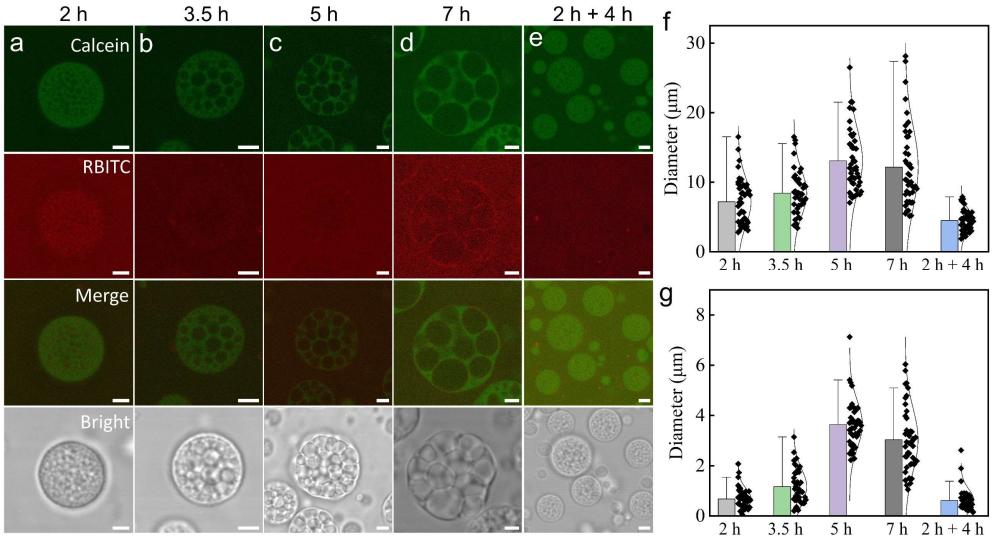

Supplementary Fig. 34. CLSM images of multi-compartmental coacervates formed by 405 nm illumination for (a) 2 h, (b) 3.5 h, (c) 5 h, and (d) 7 h. (e) The multi-compartmental coacervates in (a) are further stirred at 100 rpm for 4 h under dark condition as a control. (f) The corresponding external diameter of multi-compartmental coacervates in a-e. (g) The diameter of sub-compartments in a-e. Data are presented as mean ± s.d. (n = 44). Scale bars, 3 μm. Source data are provided as a Source Data file.

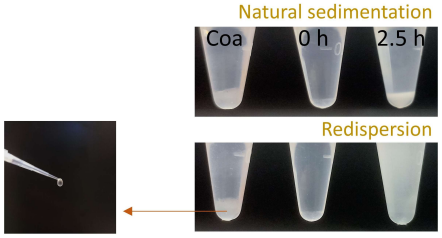

Supplementary Fig. 35. Photograph of HA/PDDA coacervates (Coa), HA/PDDA/BSA/DMAEMA coacervates (0 h) and multi-compartmental coacervates formed by 405 nm illumination for 2.5 h (2.5 h). After 24 h, HA/PDDA coacervates condense at the bottom, and the inset shows the coacervates cannot be further dispersed. HA/PDDA/BSA/DMAEMA coacervates show clear solution due to dissociation of coacervates. In contrast, the multi-compartmental coacervates can be well redispersed.

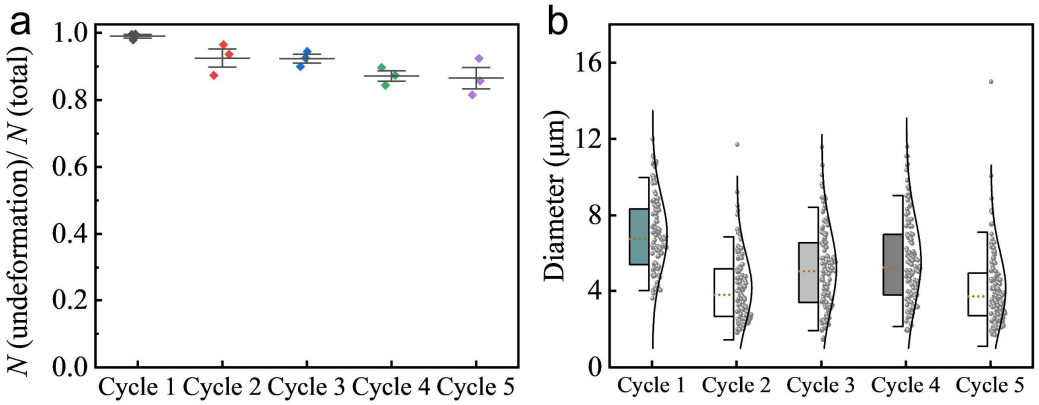

Supplementary Fig. 36. (a) Statistics of multi-compartmental coacervates undergoing five cycles of centrifugation at 300 × *g* for 1 min. *N*(undeformation) = the number of undeformed multi-compartmental coacervates, *N*(total)= the total number of multi-compartmental coacervates. Data are presented as mean ± s.d. (n = 3). (b) The corresponding diameter of multi-compartmental coacervates. Data are presented as mean ± s.d. (n = 118). Source data are provided as a Source Data file.

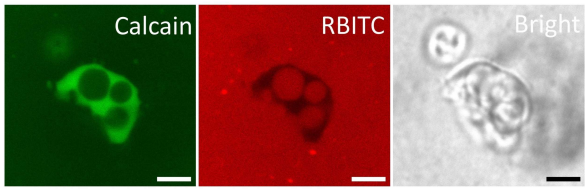

Supplementary Fig. 37. CLSM images of the multi-compartmental coacervate fragment showing robustness and stability of multi-compartmental coacervates. Scale bars, 3 μm.

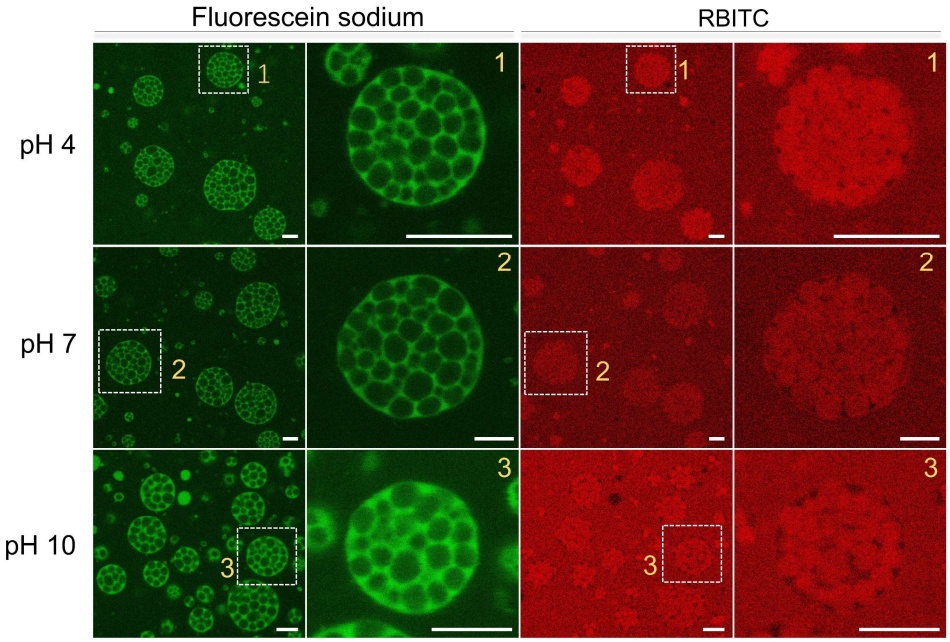

Supplementary Fig. 38. CLSM images of HA/PDDA/BSA/DMAEMA coacervates formed by 405 nm illumination for 2.5 h in the different pH solutions (PBS, 10 mM), showing the formation of the multi-compartmental coacervates in different pH solutions. Fluorescein sodium (green) is sequestrated in the coacervate matrix and RBITC (red) is encapsulated in sub-compartments. Scale bars, 5 μm.

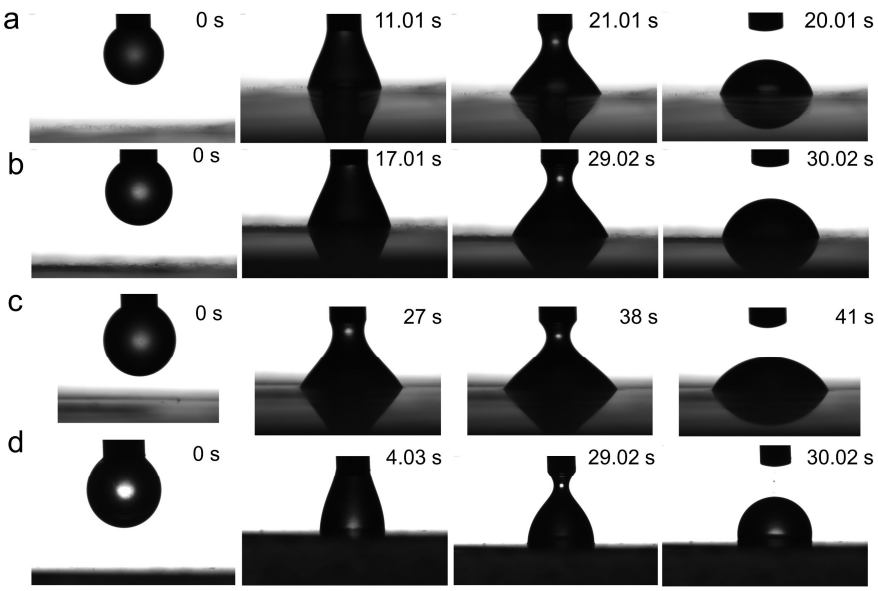

Supplementary Fig. 39. Time-dependent contour images of droplets, showing that droplets contact the surface and then break from the surface, which is used for calculation of drop adhesion force (DAF) and contact angle (θ). (a) HA/PDDA coacervate solution, (b) HA/PDDA/BSA coacervate solution, (c) HA/PDDA/BSA/DMAEMA coacervate solution (0 h) and (d) HA/PDDA/BSA/DMAEMA coacervate solution obtained by 405 nm illumination for 5 h. The substrate was prepared by adding the same solution onto the glass slide and drying naturally.

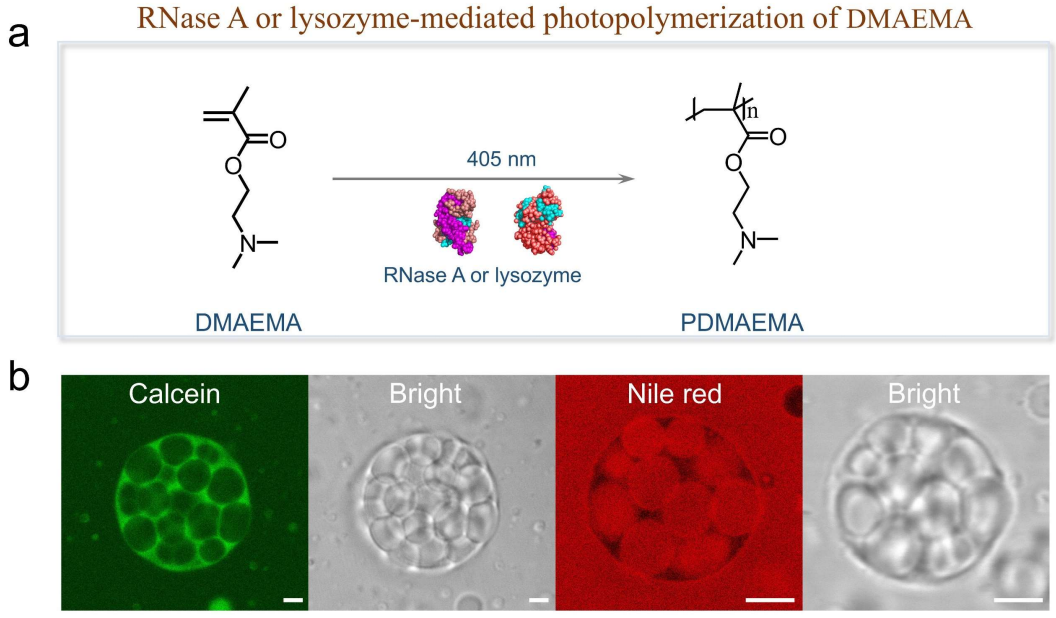

Supplementary Fig. 40. (a) Schematic illustration of RNase A or lysozyme-mediated photopolymerization of DMAEMA. (b) CLSM images of multi-compartmental coacervates induced by lysozyme-mediated photopolymerization under 405 nm for 2.5 h, showing compartmental sequestration for calcein (green) and Nile red. Scale bars, 3 μm.

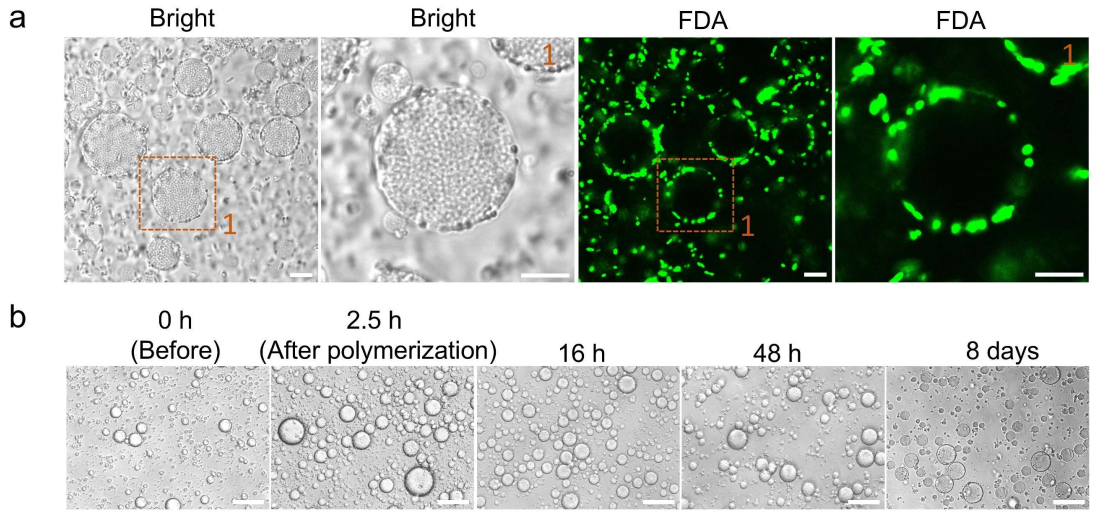

Supplementary Fig. 41. Stability of coacervates/bacteria assemblies. (a) CLSM of coacervates/bacteria assemblies containing GFP (green fluorescence), showing that the bacteria are distributed on the surface of the multi-compartmental coacervates. The coacervates/bacteria assemblies are formed by illuminating under 405 nm illumination for 2.5 h (2.5% w/v monomer content). Scale bars, 10 μm. (b) Microscopy images of coacervates/bacteria assemblies with 2.5% w/v monomer content, formed by illuminating under 405 nm illumination for 2.5 h, observed at 0 h (before), 2.5 h (after polymerization), 16 h, 48 h and 8 days, respectively. The coacervates/bacteria assemblies remain stable over 8 days. Scale bars, 50 μm.

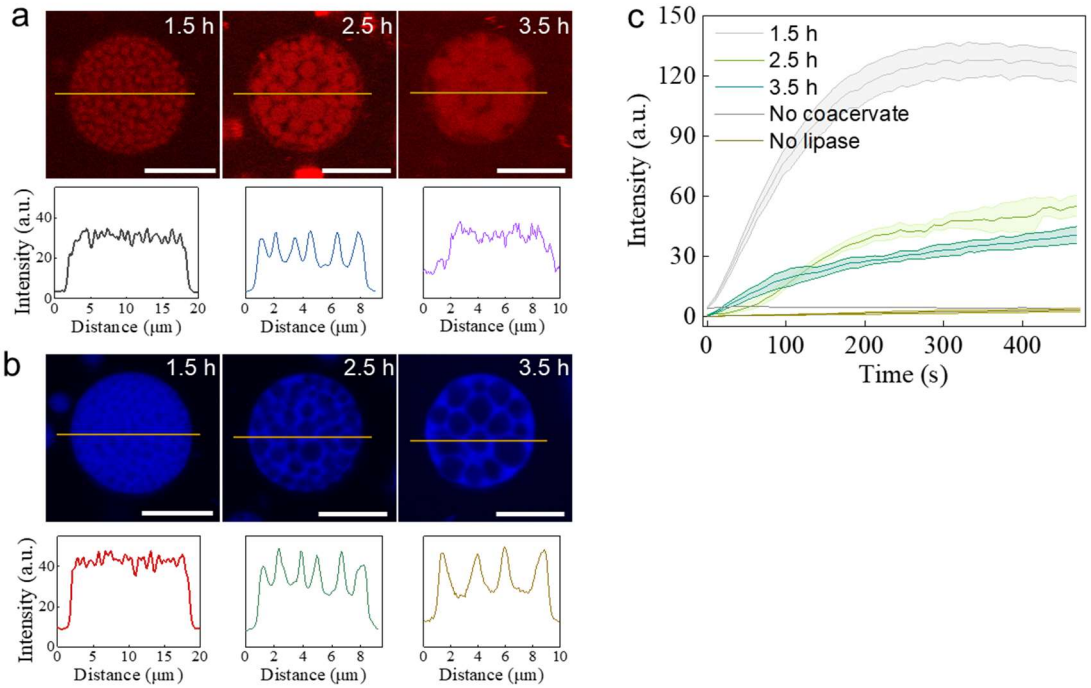

Supplementary Fig. 42. (a) CLSM images of the distribution of lipase-RBITC in multi-compartmental coacervates of different sizes obtained by polymerization under 405 nm for 1.5 h, 2.5 h and 3.5 h, respectively. The bottom is the corresponding fluorescence intensity profile, showing that lipase-RBITC was distributed in sub-compartments (red fluorescence). (b) The corresponding CLSM images of interfacial catalysis of lipase-RBITC in multi-compartmental coacervates after 400 s of catalytic reaction. The bottom is the corresponding fluorescence intensity profile, showing that the catalytic product 4-methylumbelliferone (blue fluorescence) was loaded in coacervate matrix. (c) The fluorescent intensity statistics of the catalytic product generated by interfacial catalysis of lipase-RBITC. The shaded region represents the error interval of standard deviation of the mean points. Scale bars, 5 μm. Source data are provided as a Source Data file.

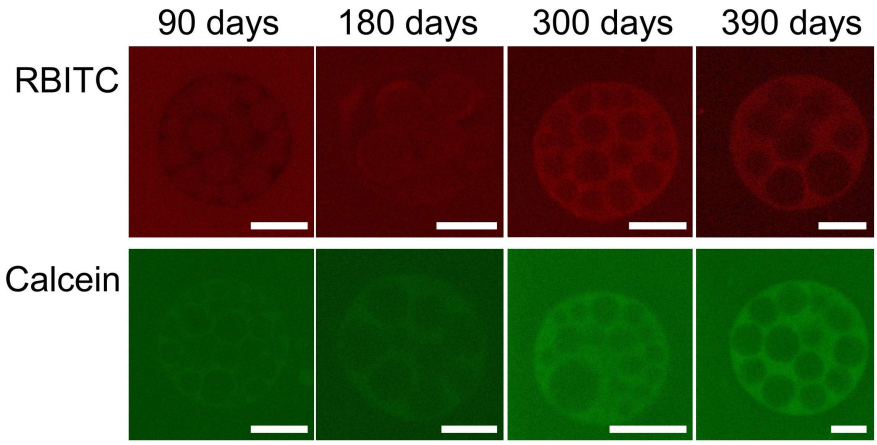

Supplementary Fig. 43. CLSM images of sequestration of multi-compartmental coacervates for calcein (green) and RBITC (red), formed by 405 nm illumination for 2.5 h and observed at 90, 180, 300 and 390 days, respectively, showing sequestration for calcein in matrix and transferred sequestration of RBITC from sub-compartments into coacervate-matrix after 300 days. Scale bars, 5 μm.

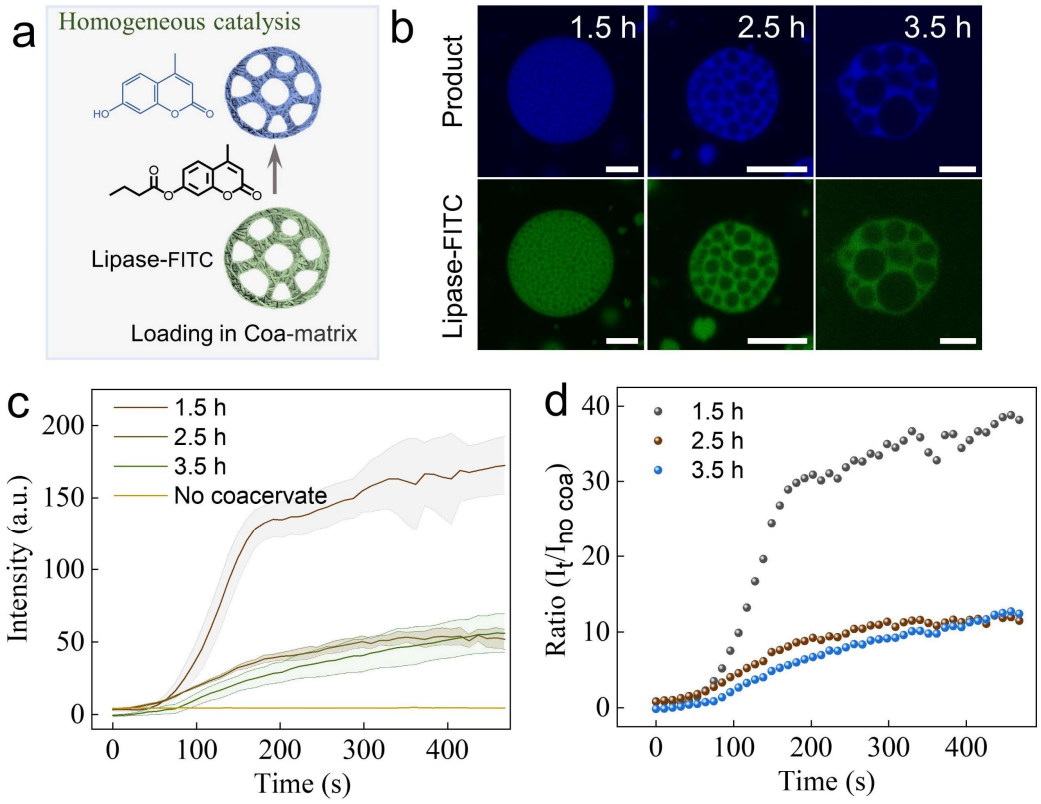

Supplementary Fig. 44. (a) Schematic illustration of homogeneous catalysis of lipase-FITC in multi-compartmental coacervates. (b) CLSM images of multi-compartmental coacervates with sub-compartments of different sizes, obtained by polymerization under 405 nm for 1.5 h, 2.5 h and 3.5 h, respectively, showing both lipase-FITC (green) and the fluorescent product 4-methylumbelliferone (blue) loaded in coacervate matrix. (c) The fluorescent intensity statistics of the catalytic product generated by homogeneous catalysis of lipase-FITC. The shaded region represents the error interval of standard deviation of the mean points. (d) The corresponding fluorescent ratio statistics of the product in multi-compartmental coacervates or no coacervates. Scale bars, 5 μm. Source data are provided as a Source Data file.

Supplementary references

1. Jinhye, et al. "Osmotically Driven Formation of Double Emulsions Stabilized by Amphiphilic Block Copolymers." *Angew. Chem. Int. Ed*. **53**, 8240 –8245 (2014)

2. Zhang, Y. et al. Osmotic-induced reconfiguration and activation in membranized coacervate-based protocells. *J. Am. Chem. Soc*. **145**, 10396-10403 (2023).